ACS APPLIED MATERIALS & INTERFACES

Letter

www.acsami.org

Ion-Exchange Route to Au−Cu_xOS Yolk−Shell Nanostructures with Porous Shells and Their Ultrasensitive H_2O_2 Detection

Lizhen Zhou, Long Kuai, Wenzheng Li, and Baoyou Geng*

College of Chemistry and Materials Science, The Key Laboratory of Functional Molecular Solids, Ministry of Education, Anhui Laboratory of Molecular-Based Materials, Anhui Normal University, Wuhu, 241000, P. R. China

Supporting Information

ABSTRACT: In this letter, Au−Cu_xOS yolk−shell nanostructures with porous shell are prepared through a facile ion exchange route from Au@Cu_2O core−shell nanostructures. The as-prepared yolk−shell nanostructures exhibit ultrasensitive enzyme-free detection of H_2O_2 molecules with higher sensitivity (50.41 $\mu A\ \mu M^{-1}$) and lower detection limit (0.01 μM) as well with excellent anti-interference capacity in comparison with both hollow Cu_xOS nanospheres and Au nanoparticles. Therefore, the obtained Au−Cu_xOS yolk−shell nanostructures have potential application in ultralow concentration enzyme-free H_2O_2 detection for biomedicine diagnosis.

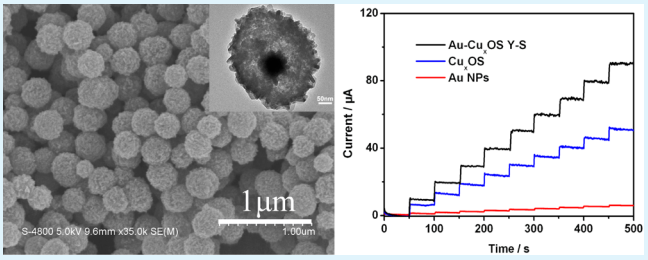

KEYWORDS: *Au−Cu_xOS yolk−shell nanostructures, ion exchange, H_2O_2 detection*

1.0. INTRODUCTION

The precise and low-scale detection of biomolecules, such as hydrogen peroxide (H_2O_2),[1] glucose,[2] amino acids etc.,[3] is of great importance in biomedicine diagnosis. Biosensor is a device that generates a physical/chemical signal, which is proportional to the concentration of the target analyte.[4] Recently, enzyme-free electrochemical sensors have been paid great attention for their excellent stability, facile operation process, and available usage in various conditions.[5] Nanoparticles-modified electrode gives rise to a great improvement for enzyme-free biosensing. Especially, some of the copper (Cu)-based semiconductor nanostructures show obviously high performance of enzyme-free biosensing. For example, Zhang et al. Prepared CuS nanoparticles assembled nanotubes for enzyme-free glucose sense with high sensitivity and low detection limit than that of conventional CuS nanotubes.[6] In addition, our group fabricated Cu_2O homogeneous yolk−shell structures and found that they possessed higher efficiency toward the detection of dopamine than solid ones.[7] Thus, the sensing performance shows highly structure-dependent properties, which strongly inspires us to design and synthesize efficient nanostructures as the candidate for enzyme-free detection of biomolecules.

Many results have confirmed a fact that yolk−shell nanostructures have outstanding performance for catalysis,[8] drug delivery[9] and lithium-ion batteries.[10] The difference between yolk−shell and core−shell nanostructure is the space between core and shell. This space can act as a nanoreactor and enhance the performance.[11] The Au@TiO_2 core−shell hollow spheres[12] and core−shell Au@CeO_2 nanocomposites[13] have been fabricated in order to avoid unstable Au NPs and let much better nanostructures come into being, so in this work, we designed and prepared a metal/semiconductor yolk−shell nanostructure, Au−Cu_xOS, for the ultrasensitive detection of H_2O_2. To confirm the biosensing advantages of the obtained Au−Cu_xOS yolk−shell nanostructure, we took enzyme-free H_2O_2 detection as a modal example. In comparison with both hollow Cu_xOS nanostructures and Au nanoparticles, Au−Cu_xOS yolk−shell nanostructure exhibited significantly enhanced sensing performance of higher sensitivity (50.41 $\mu A\ \mu M^{-1}$) and lower detection limit (0.01 μM) as well with excellent anti-interference capacity. Therefore, the Au−Cu_xOS yolk−shell nanostructures have potential application of enzyme-free ultralow concentration of H_2O_2 detection for biomedicine diagnosis.

2.0. EXPERIMENTAL SECTION

2.1. Chemicals. All the chemicals were analytic grade (AR), and were used without further purification. Hydrogen tetrachloroaurate (III) hydrate ($HAuCl_4$) was bought fromTianjin Jinbolan NobleMetal Limited

Corporation(Tianjin, China), ethanol (C_2H_5OH), hydrazine hydrate solution ($H_4N_2{\cdot}10H_2O$, 50%), copper(II) nitrate trihydrate ($Cu(NO_3)_2{\cdot}3H_2O$), and sodium sulfide ($Na_2S{\cdot}9H_2O$) were purchased from Shanghai ReagentsLimited Corporation(Shanghai, China), and polyvinylpyrrolidone (PVP, M_w = 360 000) was purchased from China Institute of NewChemical Reagents (Shanghai, China). Distilled water was used in all experiments.

2.2. Methods. *2.2.1. Preparation of Au Nanoparticles.* Under vigorous stirring, 0.40 g of PVP was added into 10 mL of deionized water and then 15 mL of 0.1 M ascorbic acid and 2 mL of 9.7 mM

Received: November 2, 2012
Accepted: November 27, 2012
Published: November 27, 2012

   dx.doi.org/10.1021/am302546d | ACS Appl. Mater. Interfaces 2012, 4, 6463−6467

$HAuCl_4$ were added into the above solution under continuous stirring for 15−20 min at room temperature. The product is centrifugated and washed with deionized water and absolute ethanol 2−3 times in turn. The obtained Au nanoparticles were dispersed in 10 mL of deionized water for further use.

2.2.2. Synthesis of Au@Cu_2O Core−Shell Nanostructure. Typically, 0.20 g of PVP and 1 mL of Au NPs solution were added into 10 mL of 10 mM Cu $(NO_3)_2{\cdot}3H_2O$ solution, 10 μL of $H_4N_2{\cdot}10H_2O$ was added to the solution, and the mixture was stirred vigorously for 2 min. The products were then collected by centrifugation, washed with deionized water and absolute ethanol several times, and dried in air at 60 ° C in a vacuum.

2.2.3. Synthesis Procedure of Au−Cu_xOS Yolk−Shell Nanostructure. The obtained Au@Cu_2O nanoparticles was dissolved into 10 mL of water, and then 0.12 g of Na_2S powder was added under vigorous stirring for 1 h to ensure they were sufficiently sulfurized, resulting in the formation of Au−Cu_xOS yolk−shell nanostructures. The products were collected by centrifugation, and washed with deionized water and absolute ethanol two times to remove the impurities. Cu_xOS nanostructures was obtained with a similar method, and the Cu_2O was prepared by a reported method.[17e]

3.0. RESULTS AND DISCUSSION

Scheme 1 illustrates the typical preparing process of Au−Cu_xOS yolk−shell nanostructure, which includes three procedures. First, Au nanoparticles (NPs) are prepared in the presence of PVP and ascorbic acid. As shown in Figure 1a, the average diameter is about 40 nm. Then, Au@Cu_2O core−shell nanostructures are prepared through the epitaxial growth of Cu_2O shell onto Au seeds as the reported method.[14] According to Figure 1b and Figure S1 in the Supporting Information, the core−shell nanostructures are well-shaped with the average diameter of 250 nm. It can be found that each Au@Cu_2O core−shell particle consists of one or two Au NPs as core. The inset of Figure 1b apparently shows the core−shell nanostructure. The thickness of Cu_2O shell is about 110 nm. Finally, Na_2S aqueous solution is introduced in order to bring sulfurization treatment of the above product and Au−Cu_xOS yolk−shell nanostructure with porous shell is formed. As depicted in Figure 1c, typical yolk−shell nanostructures were well obtained. As shown in the low-magnification SEM (Figure S2a in the Supporting Information) images, the core−shell structure is well-preserved after sulfurizing procedure. The difference is that hollow porous shell appeared instead of initial solid Cu_2O shell. The formation of yolk−shell nanostructures is because O^{2-} diffuses quicker than S^{2-} because of the larger ionic radius of S^{2-} than O^{2-}. The diameter of shell is about 240 nm, which is well agreement with that of Au@Cu_2O core−shell ones. Moreover, the shell is rough and porous with the pore diameter within 10 nm and the thickness of shell is about 25 nm (Figure 1c), which gives rise to a large specific surface area and more exposed active sites. Figure 1d presents the HRTEM image of the shell. The measured lattice distance is 0.34 nm, which is indexed into the {100} facets of CuS. Besides, the apparent lattice line indicates that the shell is well crystallized although the sulfurizing procedure is performed at room temperature.

EDX spectrum was carried out to reveal the components of the as-prepared yolk−shell nanostructure. As shown in Figure 1e, obvious Au, Cu, S, and O elements were observed, in which the signal of Au is assigned to the Au core, and that of Cu and S elements are belonged to the shell. The existence of O is owing to the remnant of Cu_2O from the initial Au@Cu_2O core−shell nanostructures. XRD pattern (Figure 1f) further confirms the chemical composition. As marked in Figure 1f, both CuS (JCPDS card: 3−898) and Cu_2O (JCPDS card: 3−1090)

Scheme 1. Schematic illustration for the Preparation of Au−Cu_xOS Yolk−Shell Nanostructures

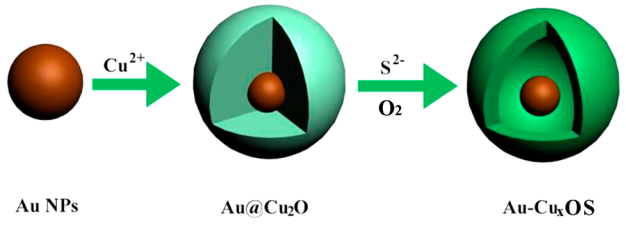

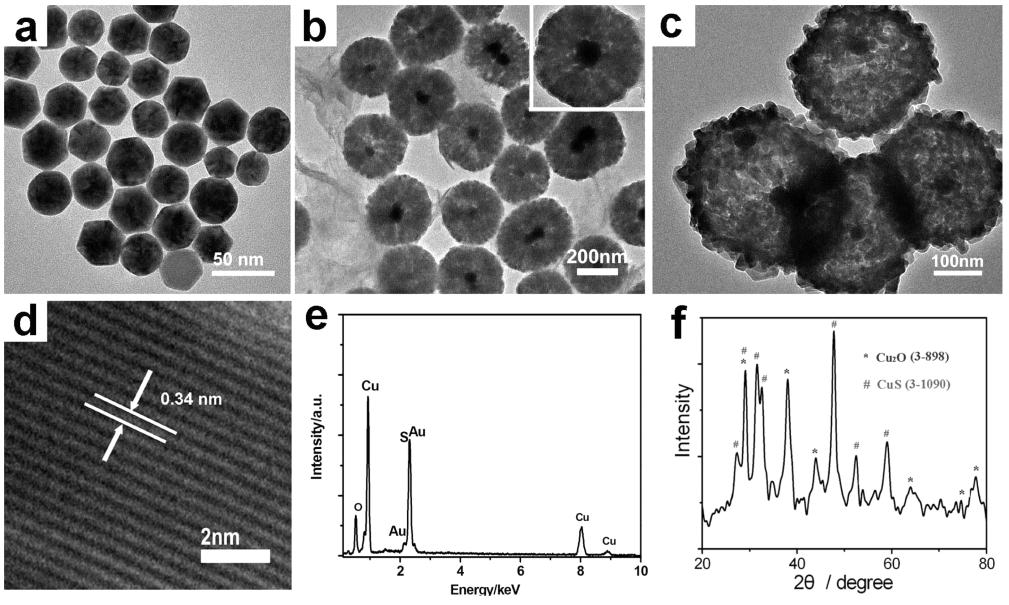

Figure 1. TEM image of (a) Au nanoparticles, (b) Au@Cu_2O core−shell and (c) Au−Cu_xOS yolk−shell nanostructures (d); HRTEM image, (e) EDX spectrum, and (f) XRD pattern of Au−Cu_xOS yolk−shell nanostructures.

dx.doi.org/10.1021/am302546d | ACS Appl. Mater. Interfaces 2012, 4, 6463−6467

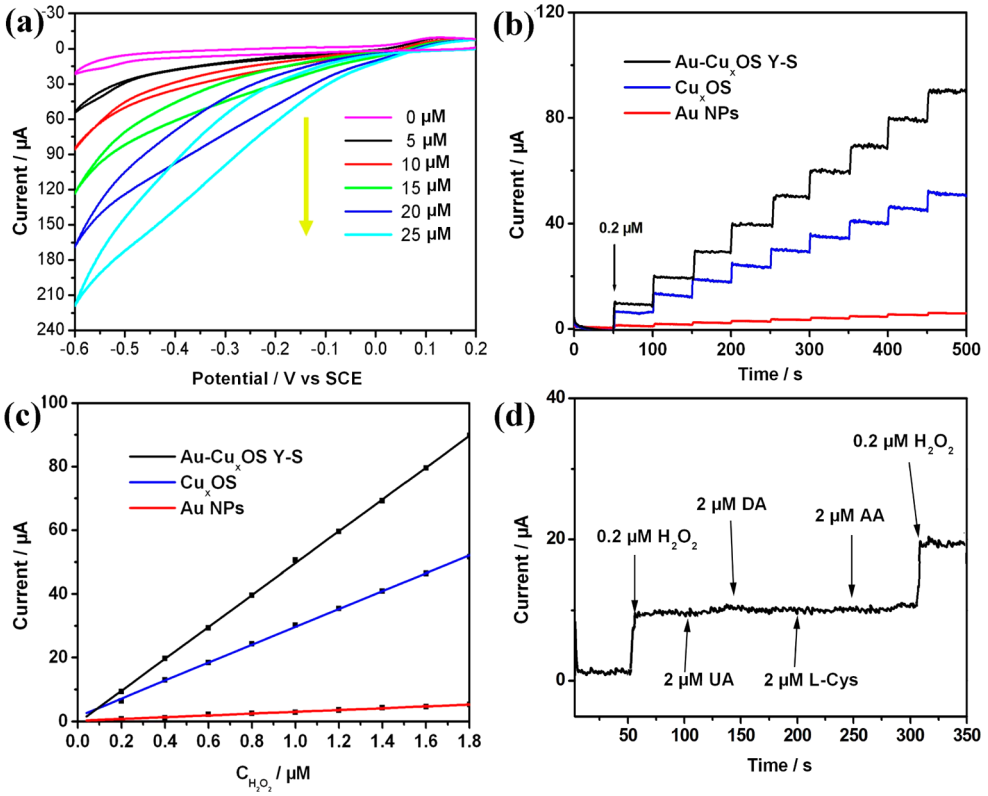

Figure 2. (a) CV curves of Au−Cu$_x$OS yolk−shell nanostructure in a series of H_2O_2 PBS solution; (b) *i*−*t* curves of Au−Cu$_x$OS yolk−shell (black), hollow Cu$_x$OS (blue) nanostructure and Au (red) nanoparticles with addition of H_2O_2, recorded at −0.2 V; (c) current curves of three samples, functioned by the concentration of H_2O_2; (d) *i*−*t* curve of Au−Cu$_x$OS yolk−shell nanostructure with addition of H_2O_2, UA, DA, L-Cys, AA, and finally H_2O_2, recorded at −0.2 V.

signals are found. The formation of CuS instead of Cu_2S is stemmed from the oxidation of O_2 at air atmosphere. Therefore, the final product is defined as Au−Cu$_x$OS yolk−shell nanostructure.

Cu-based nanostructures have been found potential application in enzyme-free biosensor.[15] metal and semiconductor nanoparticles attract much attention due to their astonishing properties and numerous possibilities for applications in sensors.[16] However, to the best of our knowledge, almost all of them are in high concentration scale for the enzyme-free detection of H_2O_2.[17] In this work, the obtained Au−Cu$_x$OS yolk−shell nanostructure was discovered to have ultrasensitive response for the enzyme-free detection of H_2O_2. For the development of an amperometric biosensor for H_2O_2, the obtained Au−Cu$_x$OS yolk−shell nanostructure was dispersed in Nafion/ethanol (0.05%) solution, a perfluorosulfonated polymer, to facilitate the modification of the polished glassy carbon (GC) electrode surface. Figure 2a shows the typical CV curves of this sensor in a series of H_2O_2 in PBS solution, where obvious reduction currents were found and the current was enlarged with the increase of concentration of H_2O_2. The chronoamperometric *i*−*t* curves were recorded to quantitatively measure the sensing performance. For comparing and studying the role of core and shell, hollow Cu$_x$OS nanostructures and Au nanoparticles were all investigated in the same condition as well. Hollow Cu$_x$OS nanostructure (shown in Figure S3 in the Supporting Information) was prepared by sulfurization of cubic Cu_2O structure, which was prepared as reported method.[14e] Figure 2b shows their representative i-t curves, which were recorded at −0.2 V. It can be obviously found that Au−Cu$_x$OS yolk−shell nanostructures have the largest current response toward H_2O_2 sensing. The current is much larger than that of both hollow Cu$_x$OS nanostructures and Au nanoparticles. On the basis of the *i*−*t* curves, the current curves functioned by concentration were obtained and shown in Figure 2c, where appeared a good linear relationship. Based in Figure 2c, the sensitivities of the three samples were obtained. It was calculated to 50.41 μA μM^{-1} for Au−Cu$_x$OS yolk−shell nanostructure, which is 1.8 times of hollow Cu$_x$OS nanostructures and 17 times of Au NPs. It is of another importance to note that the Au−Cu$_x$OS yolk−shell nanostructure modified GC electrode showed a linear region ranging from 0.01 to 5.12 μM with a high correlational coefficient of 0.999. Besides, we can find that Au NPs presented low sensing performance, but they can improve the performance of Cu$_x$OS. The structure-enhanced effect is responsible to the superior performance. First, the porous shell supplies many exposed hot spots to combine with target molecules, which is critical to highly sensing performance because the heterogeneous reaction takes place on the surface of solid phase.[18,19] The high surface-roughness factor and particular structure of the nanostructure which is suited to use as a biosensor[20] In addition, the space between core and shell acts as a important role of nanoreactor, which ensures the target molecules to be reacted as completely as possible[21] and produce larger electrochemical signals. Finally, the introduce of Au core also modifies the sensing performance, which can be obtained from the result with comparison of hollow Cu$_x$OS nanostructure. However, it is unfortunate that the important role of movable core of yolk−shell structures in catalysis is still not understood efficiently.[22] In this case, there

dx.doi.org/10.1021/am302546d | ACS Appl. Mater. Interfaces 2012, 4, 6463−6467

maybe exist synergistic effect between Au core and Cu_xOS shell. In addition, the introduce of Au can enhance its practical applications because of its excellent biocompatibility.[23,24]

Sensing selectivity is another important factor to evaluate the performance of a sensor because some electro-active species may affect the detection of H_2O_2.[25] To explore the influence of interference, uric acid (UA), dopamine (DA), L-cysteine (L-Cys), and ascorbic acid (AA) were introduced one by one during the H_2O_2 sensing process. As shown in Figure 2d, there is obvious current response after the addition of 0.2 μM H_2O_2, and no further obvious current change is observed with the subsequent addition of 2 μM UA, DA, L-Cys, and AA. Nevertheless, the current rises again with another addition of 0.2 μM H_2O_2, which indicates the high capacity of anti-interference.

4.0. CONCLUSIONS

In summary, an ultrasensitive sensor, Au−Cu_xOS yolk−shell nanostructure with porous shell has been prepared by sulfurization of Au@Cu_2O core−shell nanostructure. In comparison with hollow Cu_xOS nanostructures and Au nanoparticles, a significant improvement toward H_2O_2 sensing has been discovered. The sensitivity (50.41 $\mu A\ \mu M^{-1}$) is 1.8 times of hollow Cu_xOS nanostructures and 17 times of Au NPs. The detection limit is notably decreased to 0.01 μM and the linear region ranges from 0.01 to 5.12 μM with a high linear coefficient of 0.999. Thus, the as-prepared Au−Cu_xOS yolk−shell nanostructure may become an efficient sensor for the ultralow scale detection of H_2O_2 for medicine diagnosis.

■ ASSOCIATED CONTENT

Ⓢ Supporting Information

Additional figures and information (PDF). This material is available free of charge via the Internet at http://pubs.acs.org.

■ AUTHOR INFORMATION

Corresponding Author

*Fax: (+86)-553-3869303. E-mail: bygeng@mail.ahnu.edu.cn.

Notes

The authors declare no competing financial interest.

■ ACKNOWLEDGMENTS

This work was supported by the National Natural Science Foundation of China (20671003, 20971003, and 21271009), the Key Project of Chinese Ministry of Education (209060), the Program for New Century Excellent Talents in University (NCET 11-0888), the Science and Technological Fund of Anhui Province for Outstanding Youth (10040606Y32), the Foundation of Key Project of Natural Science of Anhui Education Committee (KJ2012A143) and the Program for Innovative Research Team at Anhui Normal University.

■ REFERENCES

(1) (a) Lei, C. X.; Hu, S. Q.; Hu, Shen, G. L.; Yu, R. Q. *Talanta* **2003**, *59*, 981−988. (b) Maji, S. K.; Dutta, A. K.; Biswas, P.; Karmakar, B.; Mondal, A.; Adhikary, B. *Sens. Actuators B* **2012**, *166−167*, 726−732. (c) Li, Z. H.; Li, D. H.; Oshita, K.; Motomizu, S. *Talanta* **2010**, *82*, 1225−1229.

(2) (a) Li, Y.; Song, Y. Y.; Yang, C.; Xia, X.-H. *Electrochem. Commun.* **2007**, *9*, 981−988. (b) Liu, Z. H.; Cho, B.; Ouyang, T. M.; Feldman, B. *Anal. Chem.* **2012**, *84*, 3403−3409. (c) Zhang, X. J.; Wang, L. L.; Ji, R.; Yu, L. T.; Wang, G. F. *Electrochem. Commun.* **2012**, *24*, 53−56.

(3) (a) Clarke, A. P.; Jangik, P.; Rocklin, R. D.; Liu, Y.; Avdalovic, N. *Anal. Chem.* **1999**, *71*, 2774−2781. (b) Luque, G. L.; Ferreyra, N. F.; Rivas, G. A. *Talanta* **2007**, *71*, 1282−1287. Deo, R. P.; Lawrence, N. S.; Wang, J. *Analyst* **2004**, *129*, 1076−1081.

(4) (a) Abo, M.; Urano, Y.; Hanaoka, K.; Terai, T.; Komatsu, T.; Nagano, T. *J. Am. Chem. Soc.* **2011**, *133*, 10629−10637. (b) Jiao, T.; leca-Bouvier, B. D.; Boullanger, P.; Blum, L. J.; Girard-Egrot, A. P. *Colloids Surf., A* **2008**, *321*, 143−146. (c) Fang, Z. H.; Lu, L. M.; Zhang, X. B.; Li, H. B.; Yang, B.; Shen, G. L.; Yu, R. Q. *Electroanalysis* **2011**, *23*, 2415−2420.

(5) (a) Retama-Retama, J.; López-Cabarcos, E.; López-Ruiz, B. *Talanta* **2005**, *68*, 99−107. (b) Burda, C.; Chen, X. B.; Narayanan, R.; El-Sayed, M. A. *Chem. Rev.* **2005**, *105*, 1025−1102. (c) Xia, Y. N.; Yang, P. D.; Sun, Y. G.; Wu, Y. Y.; Mayers, B.; Gates, B.; Yin, Y. D.; Kim, F.; Yan, Q. *Adv. Mater.* **2003**, *15*, 353−389. (d) Newman, J. D.; Turner, A. P. F. *Biosens. Bioelectron.* **2005**, *20*, 2435−2453. (e) W ilson, G. S.; Gifford, R. *Biosens. Bioelectron.* **2005**, *20*, 2388−2403. (f) Kang, X. H.; Mai, Z. B.; Zou, X. Y.; Cai, P. X.; Mo, J. Y. *Anal. Biochem.* **2007**, *369*, 71−79. (g) Wang, S. G.; Zhang, Q.; Wang, R. L.; Yoon, S. F.; Ahn, J.; Yang, J. D. *Electrochem. Commun.* **2003**, *5*, 800−803.

(6) Zhang, X. J.; Wang, G. F.; Gu, A. X.; Wei, Y.; Bin, F. *Chem. Commun.* **2008**, 5945−5947.

(7) Geng, B. Y.; Liu, J.; Zhao, Y. Y.; Wang, C. H. *CrystEngComm* **2011**, *13*, 697−701.

(8) (a) Liu, J.; Qiao, S. Z.; Chen, J. S.; Lou, X. W.; Xing, X. R.; Lu, G. Q. *Chem. Commun.* **2011**, *47*, 12578−12591. (b) Kuai, L.; Wang, S. Z.; Geng, B. Y. *Chem. Commun.* **2011**, *47*, 6093−6095.

(9) (a) Li, H. X.; Bian, Z. F.; Zhu, J.; Huo, Y. N.; Li, H.; Lu, Y. F. *J. Am. Chem. Soc.* **2007**, *129*, 8406−8407. (b) Chen, Y.; Chen, H. R.; Ma, M.; Chen, F.; Guo, L. M.; Zhang, L. X.; Shi, J. L. *J. Mater. Chem.* **2011**, *21*, 5290−5298. (c) Wu, H. X.; Liu, G.; Zhang, S. J.; Shi, J. L.; Zhang, L. X.; Chen, Y.; Chen, F.; Chen, H. R. *J. Mater. Chem.* **2011**, *21*, 3037−3045.

(10) (a) Zhang, W. M.; Hu, J.-S.; Guo, Y. G.; Zheng, S. F.; Zhong, L. S.; Song, W. G.; Wan, L. J. *Adv. Mater.* **2008**, *20*, 1160−1165. (b) Liu, J.; Xia, H.; Xue, D. F.; Lu, L. *J. Am. Chem. Soc.* **2009**, *131*, 12086−12087. (c) Wang, X.; Wu, X. L.; Guo, Y. G.; Zhong, Y. T.; Cao, X. Q.; Ma, Y.; Yao, J. N. *Adv. Funct. Mater.* **2010**, *20*, 1680−1686.

(11) (a) Liu, J.; Qiao, S. Z.; Hu, Q. H.; Lu, G. Q. *Small* **2011**, *7*, 425−443. (b) Park, J. C.; Song, H. *Nano Res* **2011**, *4*, 33−49. (c) Zhang, Q.; Lee, I.; Ge, J. P.; Zaera, F.; Yin, Y. D. *Adv. Funct. Mater.* **2010**, *20*, 2201−2214. (d) Lee, I.; Albiter, M. A.; Zhang, Q.; Ge, J. P.; Yin, Y. D.; Zaera, F. *Phys. Chem. Chem. Phys.* **2011**, *13*, 2449−2456.

(12) Du, J.; Qi, J.; Wang, D.; Tang, Z. Y. *Energy Environ.Sic* **2012**, *5*, 6914−6918.

(13) Qi, J.; Chen, J.; Li, G. D.; Li, S. X.; Gao, Y.; Tang, Z. Y. *Energy Environ. Sic.* **2012**, *5*, 8937−8941.

(14) Zhang, L.; Blom, D. A.; Wang, H. *Chem. Mater.* **2011**, *23*, 4587−4598.

(15) (a) Zhou, X. M.; Nie, H. G.; Y, Z.; Dong, Y.; Q.; Y, Z.; H, S. H. *Sens. Actuators, B* **2012**, *168*, 1−7. (b) Rahman, M. M.; Ahammad, A. J. S.; Jin, J. H.; Ahn, S. J.; Lee, J. J. *Sensors* **2010**, *10*, 4855−4886.

(16) Liu, S. Q.; Tang, Z. Y. *J. Mater. Chem.* **2010**, *20*, 24−35.

(17) (a) Song, M. J.; Hwang, S. W.; Whang, D. *Talanta* **2010**, *80*, 1648−1652. (b) Ping, J.; Ru, S.; Fan, K.; Wu, J.; Ying, Y. *Microchim. Acta* **2010**, *171*, 117−123. (c) Miao, X. M.; Yuan, R.; Chai, Y. Q.; Shi, Y. T.; Yuan, Y. Y. *J. Electroanal. Chem.* **2008**, *612*, 157−163. (d) Razmi, H.; Nasiri, H. *Electroanalysis* **2011**, *23*, 1691−1698. (e) Liu, X. W. *Langmuir* **2011**, *27*, 9100−9104.

(18) (a) Wang, L.; Yamauchi, Y. *J. Am. Chem. Soc.* **2010**, *132*, 13636−13638. (b) Zeng, H. B.; Duan, G. T.; Li, Y.; Yang, S. K.; Xu, X. X.; Cai, W. P. *Adv. Funct. Mater.* **2010**, *20*, 561−572. (c) Shi, Q. H.; Liang, H. J.; Feng, D.; Wang, J. F.; Stucky, G. D. *J. Am. Chem. Soc.* **2008**, *130*, 5034−5035. (d) Kuai, L.; Geng, B. Y.; Wang, S. Z.; Sang, Y. *Chem.—Eur. J.* **2012**, *18*, 9423−9429.

(19) Song, Y. Y.; Zhang, D.; Gao, W.; Xia, X. H. *Chem.—Eur. J.* **2005**, *11*, 2177−2182.

(20) Yuan, J. H.; Wang, K.; Xia, X. H. *Adv. Funct. Mater.* **2005**, *15*, 803−809.

(21) (a) Tan, L. F.; Chen, D.; Liu, H. Y.; Tang, F. Q. *Adv. Mater.* **2010**, *22*, 4885−4889. (b) Arnal, P. M.; Comotti, M.; Schüth, F. *Angew. Chem., Int. Ed.* **2006**, *45*, 8224−8227. (c) Pandey, A. D.; Guttel, R.; Leoni, M.; Schuth, F.; Weidenthaler, C. *J. Phys. Chem. C* **2010**, *114*, 19386−19394.
(22) Khalavka, Y.; Becker, J.; Sönnichsen, C. *J. Am. Chem. Soc.* **2009**, *131*, 1871−1872.
(23) (a) Shukla, R.; Bansal, Vi.; Chaudhary, M.; Basu, A.; Bhonde, R. R.; Sastry, M. *Langmuir* **2005**, *21*, 10644−10654. (b) Jain, P. K.; Lee, K. S.; El-Sayed, I. H.; El-Sayed, M. A. *J. Phys. Chem. B* **2006**, *110*, 7238−7248.
(24) Zhou, Y. G.; Yang, S.; Qian, Q. Y.; Xia, X. H. *Electrochem. Commun.* **2009**, *11*, 216−219.
(25) (a) Guerrier, A.; Lattanzio, V.; Palmisano, F.; Zambonin, P. G. *Biosens. Bioelectron.* **2006**, *21*, 1710−1718. (b) Carelli, D.; Centonze, D.; Palermo, C.; Quinto, M.; Rotunno, T. *Biosens. Bioelectron.* **2007**, *23*, 640−647.